Farnesyl diphosphate synthase promotes cell proliferation by regulating gene expression and alternative splicing profiles in HeLa cells

LIJUAN WANG[1], ZHIGANG CHEN[2], DONG CHEN[2], BO KAN[3], YANGFANG HE[1] and HANQING CAI[1]

[1]Department of Endocrinology, The Second Hospital of Jilin University, Changchun, Jilin 130021; [2]ABLife BioBigData Institute, Wuhan, Hubei 430075; [3]Department of Clinical Laboratory, The Second Hospital of Jilin University, Changchun, Jilin 130021, P.R. China

Received September 2, 2022; Accepted February 10, 2023

DOI: 10.3892/ol.2023.13731

Abstract. Farnesyl diphosphate synthase (FDPS), an essential enzyme involved in the mevalonate pathway, is implicated in various diseases, including multiple types of cancer. As an RNA-binding protein (RBP), FDPS is also involved in transcriptional and post-transcriptional regulation. However, to the best of our knowledge, transcriptome-wide targets of FDPS still remain unknown. In the present study, FDPS expression patterns in pan-cancer were analyzed. In addition, it was investigated how FDPS overexpression (FDPS-OE) regulates the transcriptome in HeLa cells. FDPS-OE increased the proliferation rate in HeLa cells by MTT assay. Using transcriptome-wide high throughput sequencing and bioinformatics analysis, it was found that FDPS upregulated the expression levels of genes enriched in cell proliferation and extracellular matrix organization, including the laminin subunit γ2, interferon-induced proteins with tetratricopeptide repeats 2 and matrix metallopeptidase 19 genes. According to alternative splicing (AS) analysis, FDPS modulated the splicing patterns of the bone morphogenic protein 1, semaphorin 4D, annexin A2 and sirtuin 2 genes, which are enriched in the cell cycle and DNA repair, and are related to cell proliferation. To corroborate the FDPS-regulated transcriptome findings, FDPS was overexpressed in human osteosarcoma cells. Differentially expressed genes and regulated AS genes in the cells were both validated by reverse transcription-quantitative PCR. The results suggested that, as an emerging RBP, FDPS may serve an important role in transcriptome profiles by altering gene expression and regulating AS. FDPS also affected the cell proliferation rate. These findings broaden the understanding of the molecular functions of FDPS, and the potential of FDPS as a target in therapy should be investigated.

Correspondence to: Dr Hanqing Cai, Department of Endocrinology, The Second Hospital of Jilin University, 218 Ziqiang Street, Nanguan, Changchun, Jilin 130021, P.R. China
E-mail: caihq@mail.jlu.edu.cn

Key words: farnesyl diphosphate synthase, cell proliferation, RNA sequencing, differentially expressed genes, alternative splicing

Introduction

The farnesyl diphosphate synthase (FDPS) gene encodes an enzyme involved in the mevalonate pathway that catalyzes the sequential condensation of dimethylallyl pyrophosphate with two molecules of isopentenyl pyrophosphate to form farnesyl pyrophosphate (1). FDPS contributes to the biosynthesis of cholesterol and steroid hormones, dolichols, heme A and ubiquinone, which are important intermediary metabolites that participate in numerous biological processes, including response to environmental changes. Disordered FDPS expression also leads to multiple types of cancer that threaten human health (2). For example, to investigate whether detectable FDPS activity was present in human colorectal cancer (CRC), Notarnicola *et al* (3) conducted a radiochemical assay using the tissues of 50 patients and compared the FDPS activity level in CRC tissues with that in normal surrounding mucosa. The results of the assay demonstrated that FDPS activity and its mRNA level were increased in the cancer samples compared with in normal mucosa. In addition, higher FDPS activity inhibited cellular apoptosis in CRC. Inhibiting farnesyl biosynthesis may lead to blocking of Ras signaling and the lowering of MAPK activity, thus inhibiting proliferation of glioma cells (4). FDPS also serves an important role in the apoptosis of cancer cells by blocking the JNK signaling cascade and activating mevalonate metabolism in paclitaxel-treated glioblastoma cells (5).

FDPS is also a crucial enzyme implicated in other diseases. The association between FDPS polymorphisms and osteoporosis has been extensively investigated (6-8). Due to the important functions of FDPS in the mevalonate pathway, an increasing number of studies have evaluated its potential as a drug target (9-11). Since FDPS has an affinity for bone minerals and inhibitory effects on osteoclasts, it was previously identified as a main biochemical target of the bisphonate (BP) drugs widely used to treat osteoporosis (12-15). FDPS generates isoprenoid lipids involved in the post-translational modification of small GTP-binding proteins essential for

osteoclast function (16). Therefore, inhibiting FDPS results in the antiresorptive action of BPs and prevents the biosynthesis of isoprenoid lipids, ultimately inducing cellular dysfunction and osteoclast death (17,18).

It has been demonstrated that FDPS could maintain the resorption activity of the osteoclasts (7). FDPS may promote cancer progression in PTEN-deficient prostate cancer through the GTPase/AKT axis (19). However, current studies have mainly focused on its role as a synthetase in the mevalonate pathway. A previous review study demonstrated that numerous metabolic enzymes influence RNAs or their own functions through their RNA binding activity (20). Using an RNA interactome method, researchers found that FDPS interacted with RNAs in HeLa cells (21), implying that FDPS may serve as an RNA-binding protein (RBP). By interacting with their targeted RNAs through a series of canonical RNA binding domains, RBPs serve key roles in post-transcriptional events, including alternative splicing (AS) (22), alternative polyadenylation (23,24), gene translational regulation (25) and RNA modification (26). Therefore, any disruption to RBPs that regulate crucial cellular functions may cause disease, particularly cancer cachexia (27-30). Furthermore, dysregulated AS is implicated in multiple types of human cancer, including lung and liver cancer (31), and can aberrantly activate oncogenes and cancer pathways (32). However, as an emerging RBP, how FDPS regulates AS is poorly understood and its genome-wide RNA targets have not been fully investigated.

In the present study, to identify the transcriptome-wide targets of FDPS, the FDPS gene was overexpressed in HeLa cells to investigate behavioral changes. In addition, the impact of FDPS on gene expression levels and AS was analyzed by exploring the transcriptome of the overexpression cells and control cells. To verify the findings in HeLa cells, the targeted genes were validated in human osteosarcoma (HOS) cells, which have been previously studied to investigate the molecular mechanisms of osteoporosis (33). The results revealed that FDPS extensively regulated the RNA levels and AS patterns of numerous genes that are involved in cell proliferation or are related to the cell cycle, which broadens the understanding of FDPS-mediated essential biological processes in diseases.

Materials and methods

Cell culture and transfection. The human HeLa and HOS cell lines (cat. nos. CL-0350 and CL-0360, respectively; Procell Life Science & Technology Co., Ltd.) were cultured at 37˚C with 5% CO_2 in Minimum Essential Medium (cat. no. PM150410; Procell Life Science & Technology Co., Ltd.) supplemented with 10% FBS (cat. no. 10091148; Gibco; Thermo Fisher Scientific, Inc.), 100 μg/ml streptomycin and 100 U/ml penicillin (cat. no. SV30010; HyClone; Cytiva). HeLa and HOS cells ($5x10^4$) were cultured in 24-well plates with 500 μl cell growth medium. The vector was transfected into HeLa cells using Lipofectamine® 2000 (Invitrogen; Thermo Fisher Scientific, Inc.) after cells reached 70% confluency according to the manufacturer's protocol. The cells were then incubated at 37˚C for 48 h. To construct FDPS overexpression (FDPS-OE) and empty vector control samples, HeLa and HOS cells were transfected with a FDPS-OE plasmid or empty vector (500 ng/well) using Lipofectamine® 2000 (cat. no. 11668019; Invitrogen; Thermo Fisher Scientific, Inc.) according to the manufacturer's instructions. For FDPS-OE, the coding sequence of FDPS was cloned into the pIRES-hrGFP-1a vector (cat. no. 240031; Agilent Technologies, Inc.). The plasmid was constructed according to a previously published method (34). The primer sequences for FDPS-OE construction were as follows: Forward primer, 5'-AGCCCGGGCGGATCCGAATTCATGGATTCATCCCTTACCCGC-3' and reverse primer, 5'-GTCATCCTTGTAGTCCTCGAGCTTTCTCCGCTTGTAGATTTTGC-3'. The transfection mixture was prepared at 37˚C for ~30 min, and then added to the cells for incubation for 6 h. The transfection mixture was then replaced with fresh medium and the cells were cultured until 48 h. After 48 h of transfection, the supernatant was removed from the well plate, and the cells were rinsed with PBS. The cells were then lysed with TRIzol® (cat. no. 15596-018; Ambion; Thermo Fisher Scientific, Inc.) for RNA extraction and lysed with RIPA buffer (cat. no. PR20001; Proteintech Group, Inc.) for the subsequent experiments.

Western blotting. To prepare total cell lysates, the cells were lysed on ice for 30 min using RIPA buffer (cat. no. PR20001; Proteintech Group, Inc.) containing 50 mM Tris-HCl (pH 7.4), 150 mM NaCl, 1% deoxycholate, 1% Triton X-100, 1 mM EDTA and 0.1% SDS. The samples were centrifuged (12,000 x g for 5 min at 4˚C) and 20 μl supernatant was analyzed on a 10% SDS-PAGE gel after boiling (100˚C) for 10 min. Protein concentration was determined using the BCA method, and 20 μg protein was loaded per lane. Following this, the proteins in the gel were transferred onto 0.45-mm PVDF membranes (MilliporeSigma). The membranes were blocked with 5% skimmed milk (in buffer containing 10 mM Tris pH 8.0, 150 mM NaCl and 0.05% Tween 20) for 1 h at room temperature. The membranes were incubated overnight with primary antibody at 4˚C and then incubated with HRP-conjugated secondary antibody (anti-rabbit, 1:5,000; cat. no. SA00001-2; Proteintech Group, Inc.) for 1 h at room temperature. The protein bands were visualized by chemiluminescence instrument (cat. no. 5200; Tanon Science and Technology Co., Ltd.). FDPS was detected using a monoclonal Flag antibody (1:2,000; cat. no. F7425; Sigma-Aldrich; Merck KGaA) diluted in TBS with 0.1% Tween 20. Actin (1:2,000; cat. no. AC026; ABclonal Biotech Co., Ltd.) was used as the loading control.

MTT assay. Cell proliferation or cytotoxicity was evaluated using an MTT assay. Subsequently, 25 μl MTT solution (5 mg/ml) was added to each well and the cells were incubated (37˚C) for a further 4 h. The supernatant was removed from each well after centrifugation with 2,504 x g at room temperature for 15 min. DMSO was used to dissolve the colored formazan crystals produced from the MTT added to each well (0.15 ml/well), and the optical density (OD) values were measured at 490 nm.

RNA extraction and sequencing. RNA was extracted from transfected cells using TRIzol reagent (cat. no. 15596-018; Ambion; Thermo Fisher Scientific, Inc.) and was purified twice with phenol-chloroform. RNA quality was determined by examining A260/A280 with a Nanodrop™

Table I. Reverse transcription-quantitative PCR primers used for gene expression and alternative splicing quantification.

Gene name	Primer	Sequence (5'-3')
GAPDH	Forward	CGGAGTCAACGGATTTGGTCGTAT
	Reverse	AGCCTTCTCCATGGTGGTGAAGAC
FDPS	Forward	AGGGCAATGTGGATCTTGTC
	Reverse	GAAAGAACTCCCCCATCTCC
BMP1	M/AS-Forward	ATGGCAAGTTCTGTGGTTC
	AS-Reverse	GGCCTCTTTTCTGAGAAGAAG
	M-Reverse	TCGTCCTTGTCTGAGAAGAAG
SEMA4D	M/AS-Forward	TCCACATTTCCCAGTTCTCC
	AS-Reverse	TAAGATACAGCATTTCTTCTG
	M-Reverse	CTGATGGTTTGCATTTCTTCTG
ANXA2	M/AS-Forward	CAGGTGCCTTTTGTATCC
	AS-Reverse	GCTTTCAAAAAGGGTGAAAATG
	M-Reverse	CACGGCCCAGGGTGAAAATG
SIRT2	M-Forward	AATCTGAGTCGGTCTGGCTC
	AS-Forward	AGGGTGAGAGGGGTCTGGCTC
	M/AS-Reverse	GTAGTTCTGTGCCCTATCACG

ANXA2, annexin A2; AS, alternative splicing; BMP1, bone morphogenic protein 1; FDPS, farnesyl diphosphate synthase; M, model; SEMA4D, semaphorin 4D; SIRT2, sirtuin 2.

OneCspectrophotometer (Thermo Fisher Scientific, Inc.). RNA Integrity was confirmed by 1.5% agarose gel electrophoresis. Qualified RNAs were finally quantified by Qubit3.0 with a Qubit™ RNA Broad Range Assay kit (cat. no. Q10210; Thermo Fisher Scientific, Inc.). In total, two biological replicates were prepared for both FDPS-OE and empty vector control samples. For each sample, 1 μg total RNA was used for RNA sequencing (RNA-seq) library preparation with a VAHTS Stranded mRNA-seq Library Prep Kit (cat. no. NR605-02; Vazyme Biotech Co., Ltd.). The libraries were prepared according to the manufacturer's instructions and applied to Hiseq X Ten Kit and HiSeq X/HD Reagent Kit v2.5 (300/Cycles) (Illumina, Inc.) for library construction. An Illumina HiSeq X Ten system was used for 150 nucleotide paired-end sequencing. The loading concentration was 3 ng/μl, and the concentration was finally quantified by Qubit3.0 (Thermo Fisher Scientific, Inc.). For each RNA-seq sample, the FASTX-Toolkit (version 0.0.13; http://hannonlab.cshl.edu/fastx_toolkit/) was used to remove adaptors and low-quality reads. The filtered reads were aligned onto the human genome (GRCh38 assembly) using TopHat2 v2.1.1 (35).

Differentially expressed gene (DEG) and AS analysis. The gene expression levels were calculated as fragments per kilobase of transcript per million fragments mapped (FPKM) values. The statistical power of this experimental design, calculated using RNASeqPower v1.38.0 (36), was 0.99 with two biological replicates. The Bioconductor package edgeR v3.32.1 (37) was used to screen out the DEGs between FDPS-OE and control cells. A false discovery rate (FDR) <0.05 and fold change >2 or <0.5 were set as the cut-off criteria for DEGs. A final power value of 0.90 was used to detect a 2-fold change in expression. Furthermore, Pearson's correlation analysis was performed to assess sample distance.

The AS events (ASEs) and regulated ASEs (RASEs) between the samples were defined and quantified using the ABLas pipeline as previously described (38). A total of 10 types of ASEs were detected based on the splice junction reads, including exon skipping (ES), alternative 5' splice site (A5SS), alternative 3' splice site (A3SS), intron retention, mutually exclusive exons (MXE), mutually exclusive 5' untranslated regions, mutually exclusive 3' untranslated regions, cassette exon (CE), A3SS + ES and A5SS + ES.

Fisher's exact test was used to calculate the P-value. P<0.05 was considered to indicate a statistically significant difference. The RASE ratio was calculated as the changed ratio of alternatively spliced reads and constitutively spliced reads between FDPS-OE and control samples. A RASE ratio >0.2 and P<0.05 were set as the threshold for RASE detection.

Reverse transcription-quantitative (RT-q) PCR validation of DEGs and AS events in HOS cells. To validate the RNA-seq data and assess gene overexpression, RT-qPCR was performed using FDPS-OE HOS cells for selected DEGs. The primers for RT-qPCR analysis are listed in Table I. A total of three biological replicates for FDPS-OE and control samples were used for RT-qPCR. cDNA synthesis was performed using a reverse transcription kit (cat. no. R323-01; Vazyme Biotech Co., Ltd.) at 42˚C for 5 min, 37˚C for 15 min and 85˚C for 5 sec, performed on a T100 thermocycler (Bio-Rad Laboratories, Inc.). qPCR was performed on the ABI QuantStudio 5 (Thermo Fisher Scientific, Inc.) with the following thermocycling conditions: Denaturing at 95˚C for 10 min, followed by 40 cycles of denaturing at 95˚C for 15 sec and annealing and extension at 60˚C for 1 min. PCR amplifications were performed in triplicate

for each sample. qPCR was performed on a Bio-Rad S1000 (Bio-Rad Laboratories, Inc.) with reverse transcription kit (R323-01, Vazyme, China). The PCR conditions consisted of denaturation at 95˚C for 10 min, and 40 cycles of denaturation at 95˚C for 15 sec, and annealing and extension at 60˚C for 1 min. For each sample, PCR amplifications were performed in triplicate. By normalizing the cycle threshold of the control housekeeping gene GAPDH, the expression levels of selected genes were calculated using the $2^{-\Delta\Delta Cq}$ formula (39).

In addition, RT-qPCR was also performed as aforementioned to analyze ASEs. The primers for detection of ASEs are shown in Table I. A boundary-spanning primer was used for the sequence encompassing the junction of the constitutive exon and alternative exon, and an opposing primer encompassing the constitutive exon was used for detection of alternative isoforms. The boundary-spanning primer of the alternative exon was designed according to the 'model exon' to detect model splicing or according to the 'altered exon' to detect altered splicing.

Functional annotation. The KOBAS 2.0 server (http://kobas.cbi.pku.edu.cn./) was used to carry out Gene Ontology (GO) term and Kyoto Encyclopedia of Genes and Genomes (KEGG) enrichment analyses to examine the primary functions of DEGs and differentially alternatively spliced genes (40). A hypergeometric test was used to identify the enrichment of each pathway, while the FDR (<0.05) was used to define the threshold of significance.

Other methods and statistical analysis. Ggplot2 v3.3.5 (https://github.com/tidyverse/ggplot2) was used to generate a volcano plot, heat maps and hierarchical clustering. After normalizing the reads of each gene, an in-house script (sogen) was used to visualize next-generation sequence data and genomic annotations. An unpaired two-tailed Student's t-test was conducted for comparisons between two groups using Excel (Microsoft Corporation). The data are presented as the mean ± SD of least three biological replicates, except for the RNA-seq data (two biological replicates). $P<0.05$ was considered to indicate a statistically significant difference. The Cancer Genome Atlas (TCGA) database was used to verify the FDPS expression levels and the prognostic effect of FDPS in patients with cervical cancer and other cancers via the Gene Expression Profiling Interactive Analysis 2 (GEPIA2) web server (http://gepia2.cancer-pku.cn/#index) (41). For overall survival analysis, cervical squamous cell carcinoma (CESC) patients (n=3,934) were divided into two groups by auto select best cutoff of FDPS expression level using the Kaplan-Meier Plotter web site (42).

Results

FDPS may promote proliferation in HeLa cells and is associated with multiple types of cancer. A previous RNA interactome study revealed the RNA binding ability of FDPS in HeLa cells (21), while the regulatory functions of FDPS binding to RNA remained unknown. Thus, HeLa cells were used to investigate FDPS functions on the transcriptome, and HOS cells were used to validate its potential targets. An FDPS-OE plasmid was constructed and transfected into HeLa and HOS cells. The effect of FDPS-OE in both HeLa (Fig. 1A) and HOS cells (Fig. 1B) was assessed by RT-qPCR. Western blot analysis was also conducted to confirm FDPS-OE in HeLa cells (Fig. 1C). Using an MTT assay as the detection method, it was observed that FDPS-OE resulted in an increase in OD value (Fig. 1D), suggesting that HeLa cells may proliferate more quickly in the FDPS-OE group ($P<0.01$) than in the control group. Using the GEPIA2 web server, the RNA levels of FDPS were determined to be higher in CESC tumor samples than in control samples (Fig. 1E), and patients with a higher FDPS expression level had a worse prognosis (Fig. 1F). According to GEPIA2 analysis result of TCGA data, FDPS expression was also dysregulated in other types of cancer, including colon adenocarcinoma, lymphoid neoplasm diffuse large B-cell lymphoma, liver hepatocellular carcinoma, pancreatic adenocarcinoma, rectum adenocarcinoma, thymoma, kidney chromophobe and acute myeloid leukemia (Fig. S1). These results suggest that FDPS serves important regulatory functions in multiple types of cancer.

FDPS-OE alters the global expression profiles in HeLa cells. To investigate the RNA regulatory functions of FDPS in HeLa cells, whole transcriptome sequencing (RNA-seq) experiments were performed to identify its potential targets. The polyadenylated RNAs from HeLa cells were captured after 48 h of transfection with control or FDPS-OE plasmids. For each RNA-seq sample, 70±5 million high-quality reads were obtained. Subsequently, the filtered reads were aligned onto the human genome (GRCh38 assembly) with a total aligned ratio of 91.18-92.63% and a uniquely aligned ratio of 96.73-97.61%. The uniquely aligned reads were then used for further analysis.

To compare the gene expression patterns between FDPS-OE and control samples, the expression value of each gene was calculated as FPKM, with 28,558 expressed genes being identified from the RNA-seq analysis. The overexpression of FDPS was then further validated in a parallel RNA-seq analysis using FPKM values (Fig. 2A). All expressed genes were used to calculate a correlation matrix based on Pearson's correlation coefficient (PCC) among the samples. The PCC between the FDPS-OE and control samples are presented in the diagonal of the heat map in Fig. 2B, where the two biological replicates were highly correlated.

To further investigate genes dysregulated by FDPS-OE at the transcriptional level, edgeR was used to identify DEGs between FDPS-OE and control samples. When the cut-off was set at fold change >2 or <0.5 with a 5% FDR, the number of upregulated and downregulated genes was 290 and 321, respectively, indicating that FDPS had a binary effect on transcriptional regulation (Fig. 2C; Table SI). In addition, according to the heat map analysis of the expression patterns of all DEGs, there was a clear separation between FDPS-OE and control samples and a high consistency in both datasets (Fig. 2D). In short, the aforementioned results suggest that FDPS-OE extensively regulates gene expression in HeLa cells.

To reveal the DEG-enriched functional pathways, GO and KEEG enrichment analyses were performed to annotate all 611 DEGs. The upregulated and downregulated genes were enriched in 16 and 10 GO terms, respectively. Based on the biological process terms of the GO analysis, the upregulated

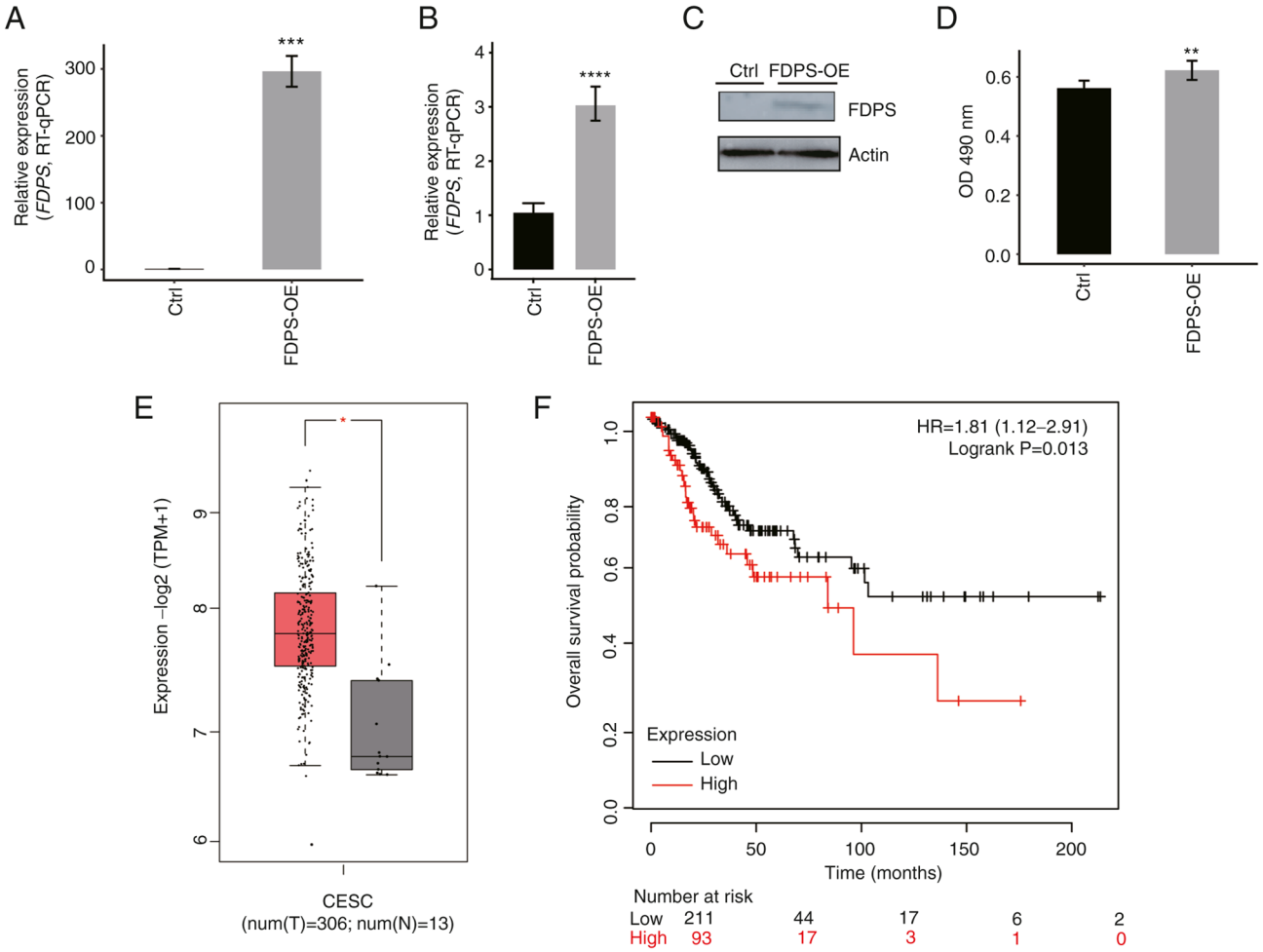

Figure 1. FDPS-OE promotes the proliferation rate of HeLa cells and influences patients with CESC. (A) FDPS-OE in HeLa cells was quantified by RT-qPCR. (B) FDPS-OE in HOS cells was quantified by RT-qPCR. (C) FDPS-OE in HeLa cells was examined by western blotting. (D) An MTT assay demonstrated that FDPS-OE promoted the proliferation of HeLa cells. (E) According to The Cancer Genome Atlas data, higher FDPS expression was observed in the tumor tissues of patients with CESC. (F) When analyzing the overall survival time, patients with CESC with higher FDPS expression were found to have a worse prognosis than patients with lower FDPS expression. Data are presented as the mean ± SD. *P<0.05, **P<0.01, ***P<0.001, ****P<0.0001. Ctrl, control; CESC, cervical squamous cell carcinoma; FDPS, farnesyl diphosphate synthase; HR, hazard ratio; num(N), number of normal tissues; num(T), number of tumor tissues; OD, optical density; OE, overexpression; RT-qPCR, reverse transcription-quantitative PCR; TPM, transcripts per million.

DEGs were mainly associated with 'positive regulation of cell proliferation', 'cytokine-mediated signaling pathway', 'immune response', 'apoptotic process' and 'extracellular matrix organization', which were important biological processes. By contrast, the downregulated genes were mainly enriched in 'transmembrane transport', 'positive regulation of transcription from RNA polymerase II promoter', 'small molecule metabolic process' and 'positive regulation of cell proliferation'(Fig. 2E). The results of the KEGG enrichment analysis are shown in Fig. 2F, the results of which were similar with that of the GO analysis.

Validation of DEGs associated with osteoporosis in HOS cells. Previous studies have demonstrated that cell proliferation (19,27), apoptosis (43,44) and migration (28) are associated with osteoporosis. Thus, several DEGs enriched in the 'positive regulation of cell proliferation', 'apoptotic process' and 'extracellular matrix organization' pathways, including *IL24*, interferon-induced proteins with tetratricopeptide repeats 2 (*IFIT2*), colony stimulating factor 2, *MMP19* and laminin subunit γ2 (*LAMC2*), were screened in HeLa cells. To determine whether these genes were also regulated by FDPS in osteoporosis cell lines, HOS cells were transfected with FDPS-OE plasmid and RT-qPCR experiments were performed. The results of these experiments demonstrated that three out of the five selected genes (*LAMC2*, *IFIT2*, and *MMP19*) exhibited similar trends after FDPS-OE, consistent with the result of the RNA-seq analysis in HeLa cells (Fig. 3).

FDPS regulates ASEs in HeLa cells. To comprehensively investigate the role of FDPS in AS regulation, RNA-seq in HeLa cells was also used to explore FDPS-meditated ASEs. The mean values of 65.3±4.0 million uniquely mapped reads were obtained from FDPS-OE and control cells, of which 40.52-41.97% were junction reads. In total, ~68.40% annotated exons (251,254 out of 367,321) were detected, together with 166,644 known splice junctions and 233,935 novel splice junctions. Using an ABLas program tool (38), 83,415 known ASEs and 61,886 novel ASEs were found.

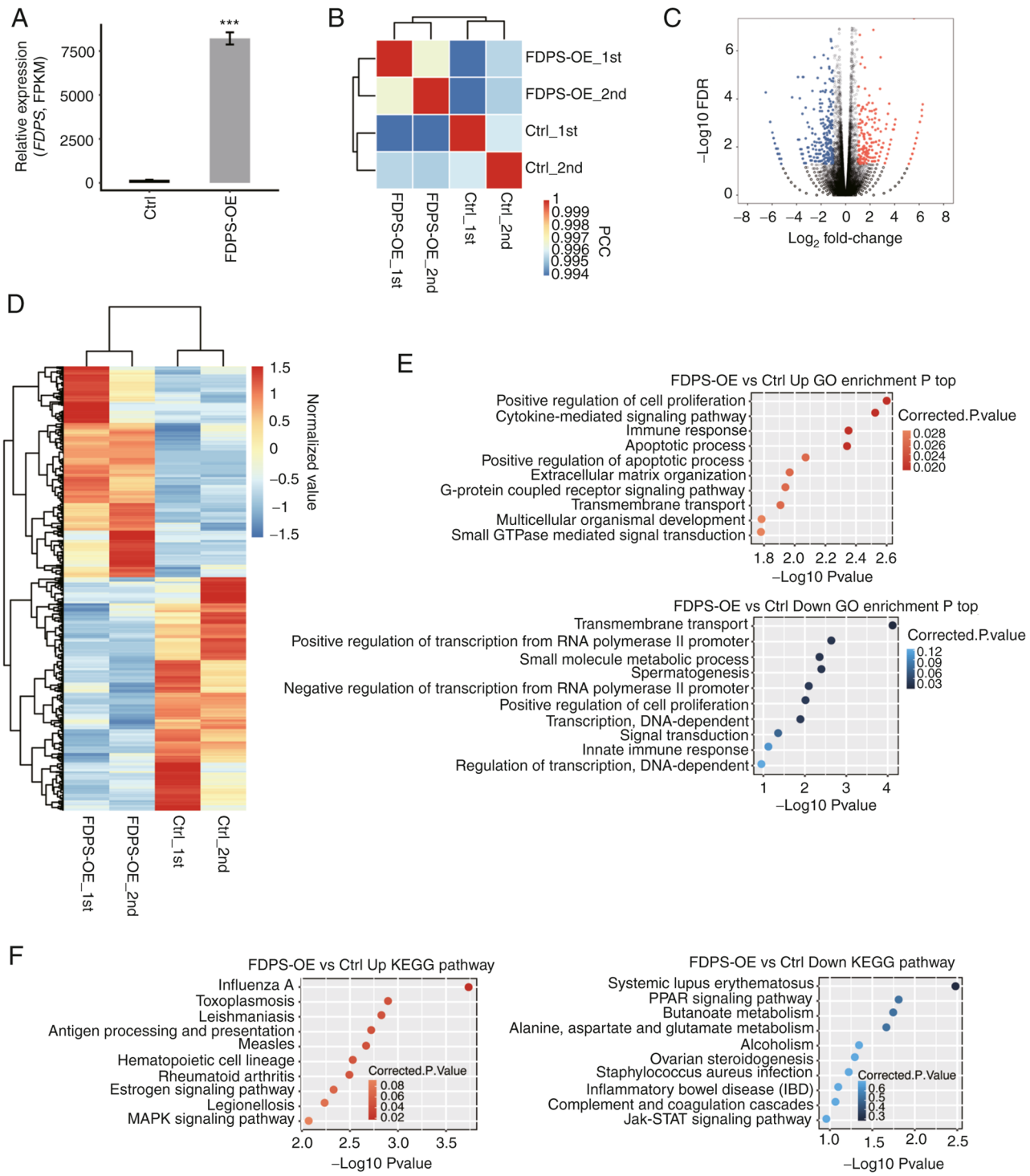

Figure 2. RNA-seq analysis of FDPS-regulated transcriptome profiles. (A) FDPS expression was quantified by RNA-seq. Data are presented as the mean ± SD. (B) Heat map showing the hierarchically clustered Pearson correlation matrix by comparing the transcript expression values of Ctrl and FDPS-OE samples. (C) Volcano plot showing the identified DEGs of FDPS-OE compared with Ctrl samples. Upregulated genes are shown in red and downregulated genes are shown in blue. (D) Hierarchical clustering heatmap showing all DEGs in the Ctrl and FDPS-OE samples. FPKM values of each gene were log2-transformed and median-centered. (E) Top 10 representative GO biological processes of upregulated and downregulated genes. (F) Top 10 representative KEGG pathways of upregulated and downregulated genes. ***P<0.001. Ctrl, control; DEGs, differentially expressed genes; FDPS, farnesyl diphosphate synthase; FDR, false discovery rate; FPKM, fragments per kilobase of transcript per million fragments mapped; GO, Gene Ontology; IBD, inflammatory bowel disease; KEGG, Kyoto Encyclopedia of Genes and Genomes; OE, overexpression; PPAR, peroxisome proliferator-activated receptor; RNA-seq, RNA sequencing.

A stringent cut-off of P<0.05 and changed ratio >0.2 was applied to identify RASEs with a high confidence (Tables SII and SIII). The most prevalent FDPS RASEs were A5SS (136 events), A3SS (95 events), CE (79 events) and ES (76 events) (Fig. 4A). These results suggested that FDPS extensively regulated ASEs in HeLa cells. By analyzing the intersection between DEGs and AS genes, it was found that four genes were shared between DEGs and regulated AS genes (RASGs). These four genes were dominated by long non-coding RNAs, including *RP1-179N16.6*, *RP5-884G6.2* and *RP11-115D19.1*

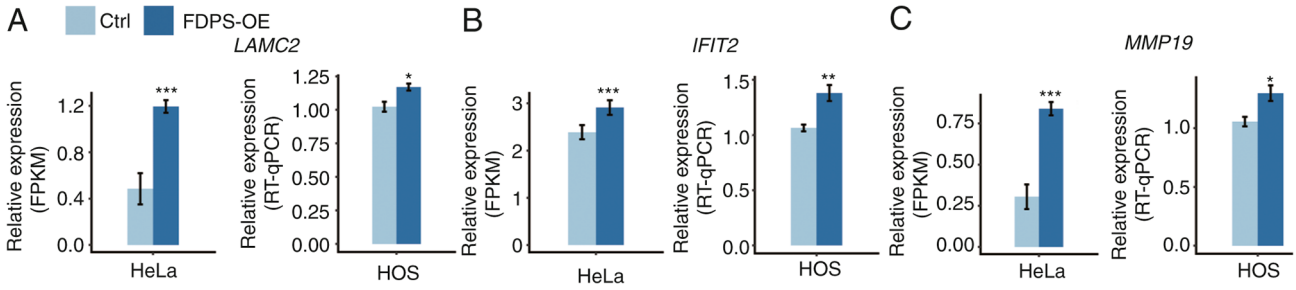

Figure 3. RT-qPCR validation of FDPS-regulated DEGs, including (A) *LAMC2*, (B) *IFIT2* and (C) *MMP19*. Relative expression levels in HeLa cells (left) and RT-qPCR validation in HOS cells (right). Student's unpaired t-test was performed to compare FDPS-OE cells with Ctrl cells. *P<0.5, **P<0.01, ***P<0.001. FDPS, farnesyl diphosphate synthase; FPKM, fragments per kilobase of transcript per million fragments mapped; RT-qPCR, reverse transcription-quantitative PCR.

(Fig. 4B). Notably, these results demonstrated that FDPS was also an RASG (Fig. 4B), suggesting that FDPS regulates its own AS pattern.

GO functional clustering analysis demonstrated that the AS genes were enriched in the 'regulation of double-strand break repair via homologous recombination', 'DNA repair' (not via homologous recombination), 'endochondral ossification', 'G2/M transition of mitotic cell cycle' and 'DNA duplex unwinding' (Fig. 4C). Enriched KEGG pathways (P<0.05) included pathways involved in 'homologous recombination', 'glycosaminoglycan biosynthesis-keratan sulfate', 'other types of *O*-glycan biosynthesis', 'glycosphingolipid biosynthesis-lacto and neolacto series' and '*N*-Glycan biosynthesis', which were important pathways (Fig. 4D).

As shown in the GO functional clustering analysis, FDPS-regulated AS genes were enriched in the 'endochondral ossification' pathway, which is associated with altering bone mass in osteoporosis (29). Therefore, three FDPS-regulated splicing events located in the alkaline phosphatase biomineralization associated, fibroblast growth factor receptor 3 and NGF1-A binding protein 1 genes were validated by RT-qPCR (data not shown). Several alternatively spliced genes were also validated by RT-qPCR in HOS cells, including bone morphogenic protein 1 (*BMP1*), semaphorin 4D (*SEMA4D*), annexin A2 (*ANXA2*) and sirtuin 2 (*SIRT2*). Although these genes were not enriched in the top 10 pathways, they are associated with osteoporosis. The RT-qPCR results of four of the seven RASGs (*BMP1*, *SEMA4D*, *ANXA2* and *SIRT2*) were consistent with the results of the transcriptome analysis in HeLa cells (Fig. 5).

Discussion

As an essential enzyme in the isoprenoid biosynthetic pathway, FDPS supplies precursors to synthesize important isoprenoids, such as sterols, ubiquinones, carotenoids and dolichols (45). Aberrant FDPS expression is associated with disease, particularly cancer. For example, elevated expression of FDPS has been found in a number of human malignant tumors, including glioblastoma (23) and prostate cancer (19). FDPS has been revealed to be a potential RBP, while the genome-wide target genes of FDPS remain to be determined (3). We hypothesize that FDPS may globally regulate gene expression and AS, eventually participating in osteoporosis through binding to RNAs.

In the present study, RNA-seq was used to perform the transcriptome analysis of FDPS-OE in HeLa cells. To the best of our knowledge, this was the first study to investigate the role of FDPS as a transcriptome regulator from a genome-wide perspective. Furthermore, FDPS-regulated DEGs and RASGs were validated in FDPS-OE HOS cells, indicating that FDPS may modulate transcriptome profiles in bone cells. FDPS has been demonstrated to promote bone resorption, and thus, is indispensable in osteoporosis development (7). In the present study, it was demonstrated that FDPS regulated the mRNA levels and the AS of genes involved in the 'positive regulation of cell proliferation', 'apoptotic process', 'extracellular matrix organization' and 'endochondral ossification' pathways, which may provide a novel perspective in understanding FDPS biology and regulatory mechanisms.

The level of cell proliferation was demonstrated to be increased significantly in FDPS-OE cells, which was consistent with the previous finding that FDPS had an important role in promoting cell proliferation (23,46). Additionally, due to FDPS-OE, several genes associated with 'positive regulation of cell proliferation', 'immune response' and 'extracellular matrix organization' pathways were upregulated, including *IFIT2*, *MMP19* and *LAMC2*, which may benefit the survival, proliferation and migration of cancer cells. IFIT2, an IFN-stimulated gene, is a tumor suppressor that inhibits proliferation and migration, while promoting the apoptosis of cancer cells in a number of tumor types (47-50). In addition to cancer, IFIT2 dysregulation has also been reported to be associated with osteoporosis. Gao *et al* (51) demonstrated that *IFIT2* serves crucial roles in the fracture repair process in osteoporosis, although the exact mechanisms remain elusive. In the present study, *IFIT2* upregulation was induced by FDPS-OE, implying novel regulating mechanisms of FDPS in osteoporosis development.

In the present study, it was demonstrated that FDPS regulated the expression of genes involved in 'extracellular matrix organization'. MMP1, MMP2, MMP9 and MMP13 are expressed in bone tissues and serve key roles in the digestion of bone matrix by osteoblasts. MMP13 is also positively associated with bone mineral density (52,53). By contrast, MMP2 and MMP9 are negatively associated with bone mineral density (22). MMP19 is also involved in the breakdown of extracellular matrix in normal physiological processes, such as embryonic development, reproduction and

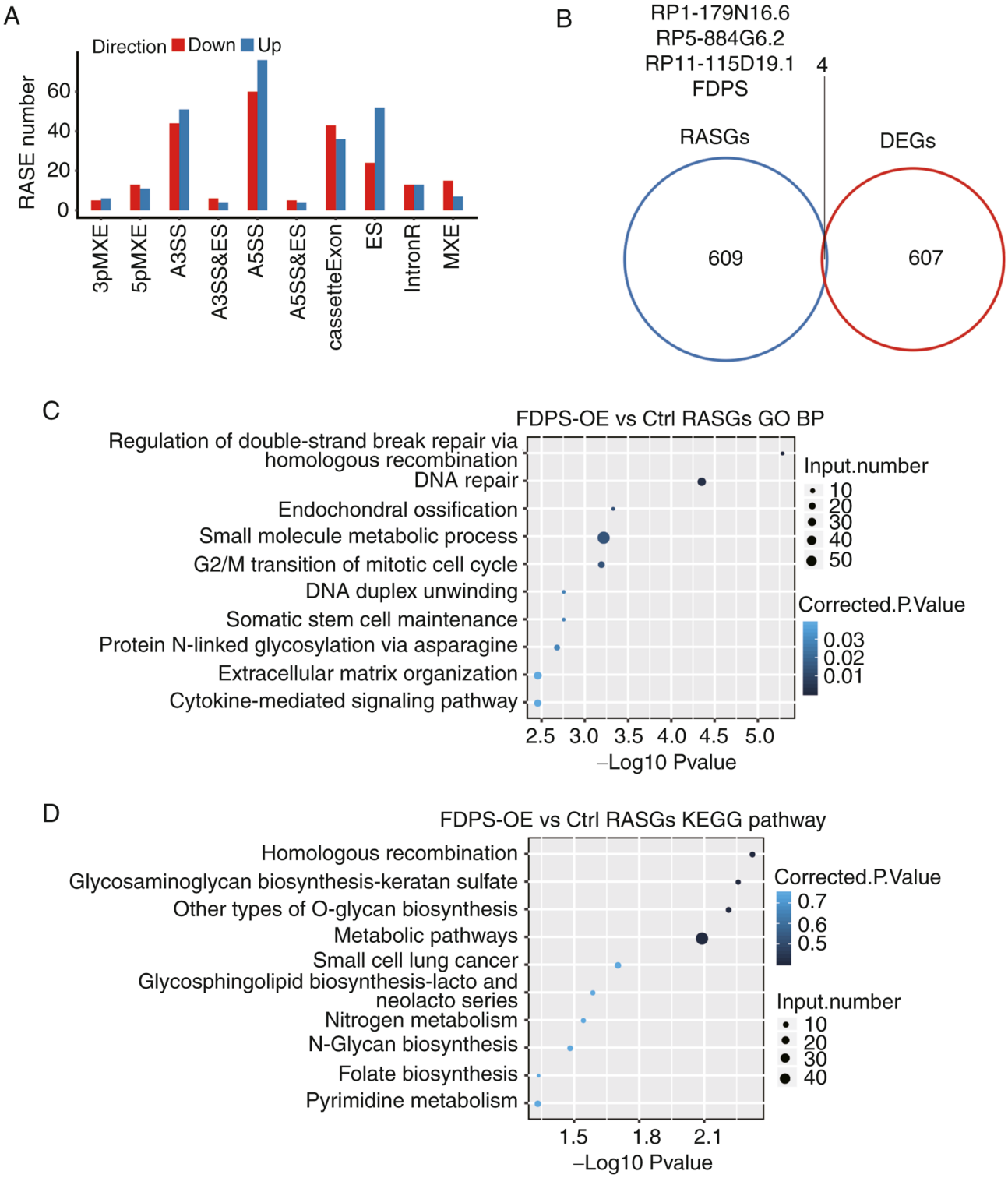

Figure 4. Identification and functional analysis of FDPS-regulated genes and ASEs. (A) Bar plot showing the classification of FDPS-regulated ASEs. (B) Venn diagram showing the overlap of FDPS-regulated DEGs and RASGs. (C) Top 10 enriched GO biological processes of FDPS-regulated alternatively spliced genes. (D) Top 10 enriched KEGG pathways of FDPS-regulated alternatively spliced genes. 3pMXE, MXE 3' untranslated regions; 5pMXE, MXE 5' untranslated regions; A3SS, alternative 3' splice site; A5SS, alternative 5' splice site; ASEs, alternative splicing events; Ctrl, control; DEGs, differentially expressed genes; ES, exon skipping; FDPS, farnesyl diphosphate synthase; GO, Gene Ontology; IntronR, intron retention; KEGG, Kyoto Encyclopedia of Genes and Genomes; MXE, mutually exclusive; RASE, regulated ASE; RASGs, regulated alternative splicing genes.

tissue remodeling (54). However, to the best of our knowledge, the function of MMP19 in osteoporosis remains unknown. Upregulation of MMP19 induced by FDPS-OE in the present study indicated that MMP19 may decrease bone mineral density in a manner analogous to MMP2 and MMP9. However, further investigation is required. LAMC2, a member of the extracellular matrix glycoprotein family, is the major component of basement membranes. *LAMC2* is involved in various biological processes, including cell adhesion, differentiation, migration, invasion, traction force and metastasis (55). *LAMC2*

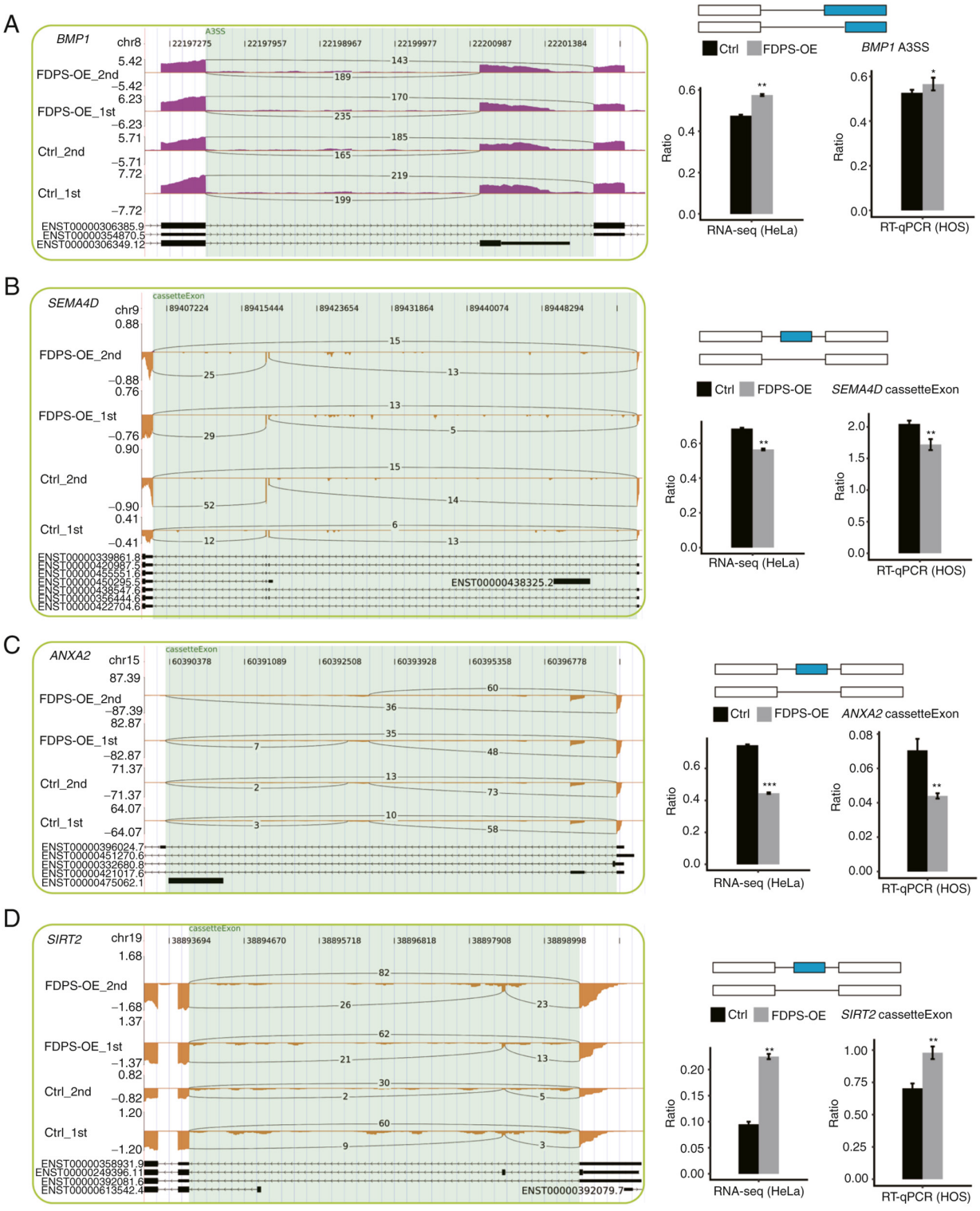

Figure 5. FDPS regulates the AS of genes involved in osteoporosis. Integrative genomics viewer (IGV)-sashimi plots showing different ASEs in four genes, including (A) *BMP1*, (B) *SEMA4D*, (C) *ANXA2* and (D) *SIRT2*. The reads distribution of each RASE is plotted in the left panel with the transcript ID and structure of each gene shown below. The schematic diagrams depict the structures of ASEs, AS1 (top) and AS2 (bottom) of top right panel. The constitutive exons are denoted by white boxes, intron sequences by a horizontal line (right; top panel) and alternative exons by blue boxes. RNA-seq quantification in HeLa cells and RT-qPCR validation of ASEs in HOS cells are shown in the bottom right panel. The data are presented as the mean ± SD. *P<0.05, **P<0.01, ***P<0.001. A3SS, alternative 3' splice site; ANXA2, annexin A2; AS, alternative splicing; ASE, AS event; BMP1, bone morphogenic protein 1; Ctrl, control; ENST, prefix of transcript ID ensembl transcript; FDPS, farnesyl diphosphate synthase; OE, overexpression; RNA-seq, RNA sequencing; RT-qPCR, reverse transcription-quantitative PCR; SEMA4D, semaphorin 4D; SIRT2, sirtuin 2.

expression was upregulated by FDPS-OE in the present study. However, to the best of our knowledge, the role of *LAMC2* in osteoporosis has not yet been reported. In summary, as an RBP, FDPS may participate in osteoporosis by regulating the expression levels of genes involved in bone mineral density or osteoclastogenesis.

AS removes pre-mRNA introns to generate mature mRNAs and is associated with the development of numerous diseases, including cancer (53), cardiovascular diseases (54) and neurological diseases (56,57). Systematic analysis has demonstrated that AS changes in tumors may represent independent oncogenic processes that greatly affect cancer transformations (58). Additionally, AS also serves important roles in skeletal diseases (59-61). The cytokine, TGF-β, which controls bone density, exists as three isoforms, with only upregulation of TGF-β3 being associated with osteoporosis in patients (62). Similarly, specific isoforms of the human calcitonin receptor and tartrate-resistant acid phosphatase are associated with osteoporosis (63,64). Taken together, these results suggest that the AS of genes is important for osteoporosis formation. However, there are relatively few studies on AS in osteoporosis (59). In the present study, large numbers of ASEs were detected in HeLa cells after FDPS-OE, including A3SS of *BMP1* and CE of *SRIT2*, *SEMA4D* and *ANXA2*. Furthermore, these RASEs were validated in FDPS-OE HOS cells, which is a popular cell line for the study of bone formation (65,66) or osteoporosis (67). Jing *et al* (68) observed an increase in bone mass density and bone volume fraction in *SIRT2* knockout rats. Their study suggested that SIRT2 serves a role in age-related bone loss, likely via regulation of osteoclastogenesis. SEMA4D, previously regarded as an axon guidance protein, has been demonstrated to inhibit bone formation (69) and promote bone resorption (70). Previously, a molecular and cellular basis of BMP1-dependent osteoporosis has been defined both in humans and in zebrafish (71,72). These findings indicate that BMP1 is essential for bone formation and stability. The *BMP1* gene encodes several isoforms, including BMP1 and mammalian tolloid, which proteolytically remove the C-terminal propetide from procollagen (72). In addition, BMP1-3, an isoform of the *BMP1* gene, is elevated in patients with acute bone fracture, and may be involved in bone repair (73). Whether these two isoforms of *BMP1* have an impact on osteoporosis formation needs further validation through knockdown studies or through overexpressing different isoforms. Another finding of the present study was that FDPS may regulate its own AS, which may be a feedback mechanism for FDPS upregulation, and thus, FDPS may regulate its own functions in HeLa cells. However, how FDPS regulates AS and gene expression has not been investigated in the present study. Experiments, such as pull-down or gel shift assays, should be performed in future studies.

In conclusion, in the present study, RNA-seq technology was applied to demonstrate how FDPS may regulate gene expression and AS in HeLa cells. It was demonstrated that genes critical in cell proliferation were upregulated by FDPS-OE. It was also demonstrated that the AS of genes implicated in the cell cycle was also regulated by FDPS. These results suggest that, as an RBP, FDPS may serve an important role in HeLa and HOS cells by modulating mRNA expression at transcriptional and post-transcriptional levels through binding to precursor mRNAs. Further studies are required to identify the molecular mechanisms in which FDPS regulates gene expression and AS, such as the regulatory mechanism of FDPS, to make up the flaws in the present study. In summary, the present study contributes to the understanding of FDPS-targeted therapies.

Acknowledgements

Not applicable.

Funding

This work was supported by The Natural Science Foundation of Jilin Province (grant no. 2018010113JC).

Availability of data and materials

The datasets generated and/or analyzed during the current study are available in the Gene Expression Omnibus repository, with accession number GSE151605 (https://www.ncbi.nlm.nih.gov/geo/query/acc.cgi?acc=GSE151605).

Authors' contributions

LW and HC contributed to the study conception and design. Material preparation, data collection and analyses were performed by BK, DC, ZC and YH. The first draft of the manuscript was written by LW, ZC and HC. LW, ZC, DC, BK, YH and HC confirm the authenticity of all the raw data. All authors have read and approved the final manuscript.

Ethics approval and consent to participate

Not applicable.

Patient consent for publication

Not applicable.

Competing interests

The authors declare that they have no competing interests.

References

1. Liang PH, Ko TP and Wang AHJ: Structure, mechanism and function of prenyltransferases. Eur J Biochem 269: 3339-3354, 2002.
2. Waller DD, Park J and Tsantrizos YS: Inhibition of farnesyl pyrophosphate (FPP) and/or geranylgeranyl pyrophosphate (GGPP) biosynthesis and its implication in the treatment of cancers. Crit Rev Biochem Mol Biol 54: 41-60, 2019.
3. Notarnicola M, Messa C, Cavallini A, Bifulco M, Tecce MF, Eletto D, Di Leo A, Montemurro S, Laezza C and Caruso MG: Higher farnesyl diphosphate synthase activity in human colorectal cancer inhibition of cellular apoptosis. Oncology 67: 351-358, 2004.
4. Bouterfa HL, Sattelmeyer V, Czub S, Vordermark D, Roosen K and Tonn JC: Inhibition of Ras farnesylation by lovastatin leads to downregulation of proliferation and migration in primary cultured human glioblastoma cells. Anticancer Res 20: 2761-2771, 2000.
5. Woo IS, Eun SY, Kim HJ, Kang ES, Kim HJ, Lee JH, Chang KC, Kim JH, Hong SC and Seo HG: Farnesyl diphosphate synthase attenuates paclitaxel-induced apoptotic cell death in human glioblastoma U87MG cells. Neurosci Lett 474: 115-120, 2010.
6. Marini F, Falchetti A, Silvestri S, Bagger Y, Luzi E, Tanini A, Christiansen C and Brandi ML: Modulatory effect of farnesyl pyrophosphate synthase (FDPS) rs2297480 polymorphism on the response to long-term amino-bisphosphonate treatment in postmenopausal osteoporosis. Curr Med Res Opin 24: 2609-2615, 2008.

7. Olmos JM, Zarrabeitia MT, Hernández JL, Sañudo C, González-Macías J and Riancho JA: Common allelic variants of the farnesyl diphosphate synthase gene influence the response of osteoporotic women to bisphosphonates. Pharmacogenomics J 12: 227-232, 2012.
8. Ciubean AD, Ungur RA, Irsay L, Ciortea VM, Borda IM, Dogaru GB, Trifa AP, Vesa SC and Buzoianu AD: Polymorphisms of FDPS, LRP5, SOST and VKORC1 genes and their relation with osteoporosis in postmenopausal Romanian women. PLoS One 14: e0225776, 2019.
9. Wiemer A, Hohl R and Wiemer D: The intermediate enzymes of isoprenoid metabolism as anticancer targets. Anticancer Agents Med Chem 9: 526-542, 2009.
10. Dunford JE, Kwaasi AA, Rogers MJ, Barnett BL, Ebetino FH, Russell RG, Oppermann U and Kavanagh KL: Structure-activity relationships among the nitrogen containing bisphosphonates in clinical use and other analogues: Time-dependent inhibition of human farnesyl pyrophosphate synthase. J Med Chem 51: 2187-2195, 2008.
11. Yang J, Zhu HH, Chen GP, Ye Y, Zhao CZ, Mou Y and Hu SJ: Inhibition of farnesyl pyrophosphate synthase attenuates angiotensin II-induced cardiac hypertrophy and fibrosis in vivo. Int J Biochem Cell Biol 45: 657-666, 2013.
12. Fontalis A and Eastell R: The challenge of long-term adherence: The role of bone turnover markers in monitoring bisphosphonate treatment of osteoporosis. Bone 136: 115336, 2020.
13. Kamimura M, Ikegami S, Mukaiyama K, Koiwai H, Nakamura Y, Taguchi A and Kato H: Additive effects of eldecalcitol in poorly responding long-term bisphosphonate treatment for osteoporosis. Osteoporos Sarcopenia 5: 57-61, 2019.
14. Kavanagh KL, Guo K, Dunford JE, Wu X, Knapp S, Ebetino FH, Rogers MJ, Russell RG and Oppermann U: The molecular mechanism of nitrogen-containing bisphosphonates as antiosteoporosis drugs. Proc Natl Acad Sci USA 103: 7829-7834, 2006.
15. LaFleur J, DuVall SL, Willson T, Ginter T, Patterson O, Cheng Y, Knippenberg K, Haroldsen C, Adler RA, Curtis JR, *et al*: Analysis of osteoporosis treatment patterns with bisphosphonates and outcomes among postmenopausal veterans. Bone 78: 174-185, 2015.
16. Coxon FP and Rogers MJ: The role of prenylated small GTP-binding proteins in the regulation of osteoclast function. Calcif Tissue Int 72: 80-84, 2003.
17. Russell RG, Watts NB, Ebetino FH and Rogers MJ: Mechanisms of action of bisphosphonates: Similarities and differences and their potential influence on clinical efficacy. Osteoporos Int 19: 733-759, 2008.
18. Jobke B, Milovanovic P, Amling M and Busse B: Bisphosphonate-osteoclasts: Changes in osteoclast morphology and function induced by antiresorptive nitrogen-containing bisphosphonate treatment in osteoporosis patients. Bone 59: 37-43, 2014.
19. Seshacharyulu P, Rachagani S, Muniyan S, Siddiqui JA, Cruz E, Sharma S, Krishnan R, Killips BJ, Sheinin Y, Lele SM, *et al*: FDPS cooperates with PTEN loss to promote prostate cancer progression through modulation of small GTPases/AKT axis. Oncogene 38: 5265-5280, 2019.
20. Castello A, Hentze MW and Preiss T: Metabolic enzymes enjoying new partnerships as RNA-binding proteins. Trends Endocrinol Metab 26: 746-757, 2015.
21. Castello A, Fischer B, Eichelbaum K, Horos R, Beckmann BM, Strein C, Davey NE, Humphreys DT, Preiss T, Steinmetz LM, *et al*: Insights into RNA biology from an atlas of mammalian mRNA-binding proteins. Cell 149: 1393-1406, 2012.
22. Li H, Xie S, Liu X, Wu H, Lin X, Gu J, Wang H and Duan Y: Matrine alters microRNA expression profiles in SGC-7901 human gastric cancer cells. Oncol Rep 32: 2118-2126, 2014.
23. Abate M, Laezza C, Pisanti S, Torelli G, Seneca V, Catapano G, Montella F, Ranieri R, Notarnicola M, Gazzerro P, *et al*: Deregulated expression and activity of farnesyl diphosphate synthase (FDPS) in glioblastoma. Sci Rep 7: 14123, 2017.
24. Chatrikhi R, Mallory MJ, Gazzara MR, Agosto LM, Zhu WS, Litterman AJ, Ansel KM and Lynch KW: RNA binding protein CELF2 regulates signal-induced alternative polyadenylation by competing with enhancers of the polyadenylation machinery. Cell Rep 28: 2795-2806.e3, 2019.
25. Fuller K, Owens JM, Jagger CJ, Wilson A, Moss R and Chambers TJ: Macrophage colony-stimulating factor stimulates survival and chemotactic behavior in isolated osteoclasts. J Exp Med 178: 1733-1744, 1993.
26. Shinoda K, Suda A, Otonari K, Futaki S and Imanishi M: Programmable RNA methylation and demethylation using PUF RNA binding proteins. Chem Commun (Camb) 56: 1365-1368, 2020.
27. Fagoonee S, Picco G, Orso F, Arrigoni A, Longo DL, Forni M, Scarfò I, Cassenti A, Piva R, Cassoni P, *et al*: The RNA-binding protein ESRP1 promotes human colorectal cancer progression. Oncotarget 8: 10007-10024, 2017.
28. Rauwel B, Degboé Y, Diallo K, Sayegh S, Baron M, Boyer JF, Constantin A, Cantagrel A and Davignon JL: Inhibition of osteoclastogenesis by the RNA-binding protein QKI5: A novel approach to protect from bone resorption. J Bone Miner Res 35: 753-765, 2020.
29. Kang MH, Jeong KJ, Kim WY, Lee HJ, Gong G, Suh N, Győrffy B, Kim S, Jeong SY, Mills GB and Park YY: Musashi RNA-binding protein 2 regulates estrogen receptor 1 function in breast cancer. Oncogene 36: 1745-1752, 2017.
30. Sherman EJ, Mitchell DC and Garner AL: The RNA-binding protein SART3 promotes miR-34a biogenesis and G1 cell cycle arrest in lung cancer cells. J Biol Chem 294: 17188-17196, 2019.
31. Wang E and Aifantis I: RNA splicing and cancer. Trends Cancer 6: 631-644, 2020.
32. Chen J and Weiss WA: Alternative splicing in cancer: Implications for biology and therapy. Oncogene 34: 1-14, 2015.
33. Sugiyama M, Kodama T, Konishi K, Abe K, Asami S and Oikawa S: Compactin and simvastatin, but not pravastatin, induce bone morphogenetic protein-2 in human osteosarcoma cells. Biochem Biophys Res Commun 271: 688-692, 2000.
34. Tu Y, Wu X, Yu F, Dang J, Wang J, Wei Y, Cai Z, Zhou Z, Liao W, Li L and Zhang Y: Tristetraprolin specifically regulates the expression and alternative splicing of immune response genes in HeLa cells. BMC Immunol 20: 13, 2019.
35. Kim D, Pertea G, Trapnell C, Pimentel H, Kelley R and Salzberg SL: TopHat2: Accurate alignment of transcriptomes in the presence of insertions, deletions and gene fusions. Genome Biol 14: R36, 2013.
36. Therneau T, Hart S and Kocher J: Calculating samplesSize estimates for RNA Seq studies. R package version 1.36.0, 2022.
37. Robinson MD, McCarthy DJ and Smyth GK: edgeR: A bioconductor package for differential expression analysis of digital gene expression data. Bioinformatics 26: 139-140, 2010.
38. Xia H, Chen D, Wu Q, Wu G, Zhou Y, Zhang Y and Zhang L: CELF1 preferentially binds to exon-intron boundary and regulates alternative splicing in HeLa cells. Biochim Biophys Acta Gene Regul Mech 1860: 911-921, 2017.
39. Livak KJ and Schmittgen TD: Analysis of relative gene expression data using real-time quantitative PCR and the 2(-Delta Delta C(T)) method. Methods 25: 402-408, 2001.
40. Xie C, Mao X, Huang J, Ding Y, Wu J, Dong S, Kong L, Gao G, Li CY and Wei L: KOBAS 2.0: A web server for annotation and identification of enriched pathways and diseases. Nucleic Acids Res 39 (Web Server Issue): W316-W322, 2011.
41. Tang Z, Kang B, Li C, Chen T and Zhang Z: GEPIA2: An enhanced web server for large-scale expression profiling and interactive analysis. Nucleic Acids Res 47 (W1): W556-W560, 2019.
42. Nagy Á, Munkácsy G and Győrffy B: Pancancer survival analysis of cancer hallmark genes. Sci Rep 11: 6047, 2021.
43. Fujiwara T, Zhou J, Ye S and Zhao H: RNA-binding protein Musashi2 induced by RANKL is critical for osteoclast survival. Cell Death Dis 7: e2300, 2016.
44. Li X, Ominsky MS, Villasenor KS, Niu QT, Asuncion FJ, Xia X, Grisanti M, Wronski TJ, Simonet WS and Ke HZ: Sclerostin antibody reverses bone loss by increasing bone formation and decreasing bone resorption in a rat model of male osteoporosis. Endocrinology 159: 260-271, 2018.
45. Dhar MK, Koul A and Kaul S: Farnesyl pyrophosphate synthase: A key enzyme in isoprenoid biosynthetic pathway and potential molecular target for drug development. N Biotechnol 30: 114-123, 2013.
46. Ishimoto K, Tachibana K, Hanano I, Yamasaki D, Nakamura H, Kawai M, Urano Y, Tanaka T, Hamakubo T, Sakai J, *et al*: Sterol-regulatory-element-binding protein 2 and nuclear factor Y control human farnesyl diphosphate synthase expression and affect cell proliferation in hepatoblastoma cells. Biochem J 429: 347-357, 2010.
47. Shen H, Zhan M, Zhang Y, Huang S, Xu S, Huang X, He M, Yao Y, Man M and Wang J: PLZF inhibits proliferation and metastasis of gallbladder cancer by regulating IFIT2. Cell Death Dis 9: 71, 2018.

48. Chen L, Zhai W, Zheng X, Xie Q, Zhou Q, Tao M, Zhu Y, Wu C and Jiang J: Decreased IFIT2 expression promotes gastric cancer progression and predicts poor prognosis of the patients. Cell Physiol Biochem 45: 15-25, 2018.
49. Ohsugi T, Yamaguchi K, Zhu C, Ikenoue T and Furukawa Y: Decreased expression of interferon-induced protein 2 (IFIT2) by Wnt/β-catenin signaling confers anti-apoptotic properties to colorectal cancer cells. Oncotarget 8: 100176-100186, 2017.
50. Su W, Xiao W, Chen L, Zhou Q, Zheng X, Ju J, Jiang J and Wang Z: Decreased IFIT2 expression in human non-small-cell lung cancer tissues is associated with cancer progression and poor survival of the patients. Onco Targets Ther 12: 8139-8149, 2019.
51. Gao F, Xu F, Wu D, Cheng J and Xia P: Identification of novel genes associated with fracture healing in osteoporosis induced by Krm2 overexpression or Lrp5 deficiency. Mol Med Rep 15: 3969-3976, 2017.
52. Paiva KB and Granjeiro JM: Bone tissue remodeling and development: Focus on matrix metalloproteinase functions. Arch Biochem Biophys 561: 74-87, 2014.
53. Mazur CM, Woo JJ, Yee CS, Fields AJ, Acevedo C, Bailey KN, Kaya S, Fowler TW, Lotz JC, Dang A, *et al*: Osteocyte dysfunction promotes osteoarthritis through MMP13-dependent suppression of subchondral bone homeostasis. Bone Res 7: 34, 2019.
54. Jara P, Calyeca J, Romero Y, Plácido L, Yu G, Kaminski N, Maldonado V, Cisneros J, Selman M and Pardo A: Matrix metalloproteinase (MMP)-19-deficient fibroblasts display a profibrotic phenotype. Am J Physiol Lung Cell Mol Physiol 308: L511-L522, 2015.
55. Garg M, Braunstein G and Koeffler HP: LAMC2 as a therapeutic target for cancers. Taylor & Francis, pp979-982, 2014.
56. Vuong CK, Black DL and Zheng S: The neurogenetics of alternative splicing. Nat Rev Neurosci 17: 265-281, 2016.
57. Raj T, Li YI, Wong G, Humphrey J, Wang M, Ramdhani S, Wang YC, Ng B, Gupta I, Haroutunian V, *et al*: Integrative transcriptome analyses of the aging brain implicate altered splicing in Alzheimer's disease susceptibility. Nat Genet 50: 1584-1592, 2018.
58. Climente-Gonzalez H, Porta-Pardo E, Godzik A and Eyras E: The functional impact of alternative splicing in cancer. Cell Rep 20: 2215-2226, 2017.
59. Fan X and Tang L: Aberrant and alternative splicing in skeletal system disease. Gene 528: 21-26, 2013.
60. Han Y, Wang D, Guo J, Xiong Q, Li P, Zhou YA and Zhao B: A novel splicing pathogenic variant in COL1A1 causing osteogenesis imperfecta (OI) type I in a Chinese family. Mol Genet Genomic Med 8: e1366, 2020.
61. Kimura T, Lueck JD, Harvey PJ, Pace SM, Ikemoto N, Casarotto MG, Dirksen RT and Dulhunty AF: Alternative splicing of RyR1 alters the efficacy of skeletal EC coupling. Cell Calcium 45: 264-274, 2009.
62. Grainger DJ, Percival J, Chiano M and Spector TD: The role of serum TGF-beta isoforms as potential markers of osteoporosis. Osteoporos Int 9: 398-404, 1999.
63. Beaudreuil J, Taboulet J, Orcel P, Graulet AM, Denne MA, Baudoin C, Jullienne A and De Vernejoul MC: Calcitonin receptor mRNA in mononuclear leucocytes from postmenopausal women: Decrease during osteoporosis and link to bone markers with specific isoform involvement. Bone 27: 161-168, 2000.
64. Janckila AJ, Takahashi K, Sun SZ and Yam LT: Tartrate-resistant acid phosphatase isoform 5b as serum marker for osteoclastic activity. Clin Chem 47: 74-80, 2001.
65. Wang L, Park P, La Marca F, Than K, Rahman S and Lin CY: Bone formation induced by BMP-2 in human osteosarcoma cells. Int J Oncol 43: 1095-1102, 2013.
66. Anderson PH, Atkins GJ, Findlay DM, Oloughlin PD, Welldon K, Vincent C and Morris HA: RNAi-mediated silencing of CYP27B1 abolishes 1,25(OH)2D3 synthesis and reduces osteocalcin and CYP24 mRNA expression in human osteosarcoma (HOS) cells. J Steroid Biochem Mol Biol 103: 601-605, 2007.
67. Trost Z, Trebse R, Prezelj J, Komadina R, Logar DB and Marc J: A microarray based identification of osteoporosis-related genes in primary culture of human osteoblasts. Bone 46: 72-80, 2010.
68. Jing Y, Zhou Y, Zhou F, Wang X, Tao B, Sun L, Liu J and Zhao H: SIRT2 deficiency prevents age-related bone loss in rats by inhibiting osteoclastogenesis. Cell Mol Biol (Noisy-le-grand) 65: 66-71, 2019.
69. Negishi-Koga T, Shinohara M, Komatsu N, Bito H, Kodama T, Friedel RH and Takayanagi H: Suppression of bone formation by osteoclastic expression of semaphorin 4D. Nat Med 17: 1473-1480, 2011.
70. Terpos E, Ntanasis-Stathopoulos I, Christoulas D, Bagratuni T, Bakogeorgos M, Gavriatopoulou M, Eleutherakis-Papaiakovou E, Kanellias N, Kastritis E and Dimopoulos MA: Semaphorin 4D correlates with increased bone resorption, hypercalcemia, and disease stage in newly diagnosed patients with multiple myeloma. Blood Cancer J 8: 42, 2018.
71. Asharani P, Keupp K, Semler O, Wang W, Li Y, Thiele H, Yigit G, Pohl E, Becker J, Frommolt P, *et al*: Attenuated BMP1 function compromises osteogenesis, leading to bone fragility in humans and zebrafish. Am J Hum Genet 90: 661-674, 2012.
72. Martínez-Glez V, Valencia M, Caparrós-Martín JA, Aglan M, Temtamy S, Tenorio J, Pulido V, Lindert U, Rohrbach M, Eyre D, *et al*: Identification of a mutation causing deficient BMP1/mTLD proteolytic activity in autosomal recessive osteogenesis imperfecta. Hum Mutat 33: 343-350, 2012.
73. Grgurevic L, Macek B, Mercep M, Jelic M, Smoljanovic T, Erjavec I, Dumic-Cule I, Prgomet S, Durdevic D, Vnuk D, *et al*: Bone morphogenetic protein (BMP)1-3 enhances bone repair. Biochem Biophys Res Commun 408: 25-31, 2011.